Using X-ray measurements to assess uncertainties in plasma temperature and impurity profiles in tokamaks

A. Jardin[1]*, K. Król[1], D. Mazon[2], J. Bielecki[1], D. Dworak[1], D. Guibert[2], Y. Peysson[2], M. Scholz[1] and J. Walkowiak[1]

[1] *Institute of Nuclear Physics Polish Academy of Sciences (IFJ PAN), PL-31-342, Krakow, Poland.*

[2] *CEA, IRFM, F-13108 Saint-Paul-lez-Durance, France.*

*Corresponding author: axel.jardin@ifj.edu.pl

In tokamaks, the local X-ray plasma emissivity results from the contribution of several plasma parameters, i.e. electron temperature, density and concentration of impurities in multiple ionization states. In particular, the impurity core concentration can be estimated from the emissivity in the soft X-ray (SXR) range 0.1 – 20 keV, while information about suprathermal electrons is obtained in the hard X-ray (HXR) range 20 keV – 200 keV [1]. Estimating tungsten (W) concentration is subject to uncertainties as it requires accurate knowledge of plasma temperature, magnetic equilibrium, atomic processes leading to its cooling factor and diagnostic spectral response [2]. When other plasma parameters are known, the W impurity density can be reconstructed in the core with the help of SXR tomographic tools [3], using:

$$n_W = \frac{\varepsilon_{\mathrm{SXR}}^{\eta} - \sum_{S \neq W} \varepsilon_S^{\eta}}{n_e . L_W^{\eta}(T_e)}, \tag{1}$$

where $\varepsilon_{\mathrm{SXR}}^{\eta}$ denotes the reconstructed SXR emissivity, $\sum_{S \neq W} \varepsilon_S^{\eta}$ the contribution from the background plasma and other impurities, and L_W^{η} the SXR-filtered W cooling factor, assuming a weak dependency to density and local W transport $L_W^{\eta}(T_e, n_e, \vec{\Gamma}_W) \approx L_W^{\eta}(T_e)$. Nevertheless, in the case of a significant suprathermal electron fraction e.g. due to RF heating, electron temperature estimation from ECE measurements can become a challenging task [4].

Therefore, the goal of this contribution is to establish a methodology to assess the uncertainty in the core T_e and $c_W = n_W / n_e$ based on several X-ray measurements. The strategy is to define a grid of ($T_{e,0}$, $c_{W,0}$) candidates, keeping the same radial shape, and identify the ones having the highest consistency with multiple line-integrated measurements in different energy bands. The method is at first tested on well-known synthetic profiles in an arbitrary tokamak geometry [3] to study the capabilities of the approach. W line emission is estimated thanks to the Photon Emissivity Coefficients (PEC) provided by Open-ADAS [5]. A synthetic line-integrated SXR spectrum emitted by a plasma containing W impurities ($c_W = 10^{-4}$) is presented in Fig. 1, where three spectral regions are identified: 0 - 1 keV and 1 - 5 keV dominated by line emission and a continuous part around 5 – 20 keV. A typical silicon diode + 50μm Be spectral response is shown as an example.

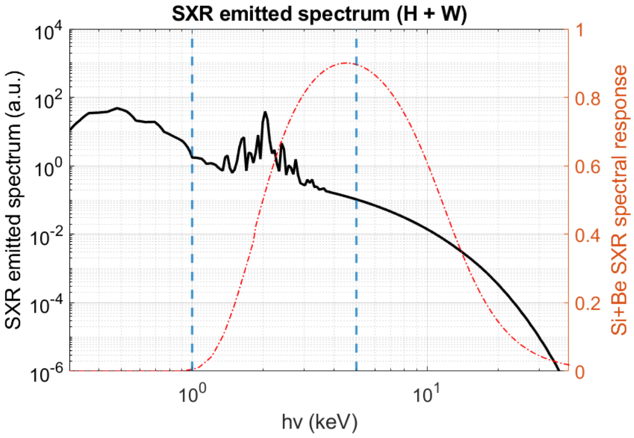

Figure 1. Simulated line-integrated emitted SXR spectrum from the plasma [3] with W impurities.

The simulated 2D emissivity remapped onto a magnetic equilibrium, in the three defined spectral ranges, is depicted in Fig. 2. The range 0.1 – 1 keV carries more information about the plasma edge while the two ranges > 1 keV contain more information about the core.

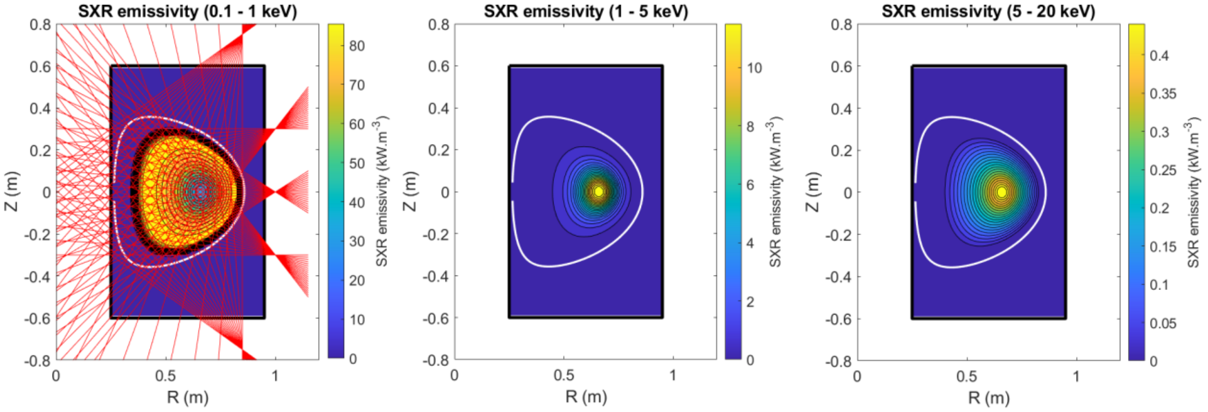

Figure 2. Synthetic plasma 2D emissivity integrated in the three defined spectral ranges.

The measurements integrated over every line-of-sight (LoS) of the five defined cameras, in each of these three spectral ranges, can be obtained by definition of the forward problem:

$$f_i^\eta = \int_{LoS} \varepsilon^\eta(R,Z)dr_i + \tilde{f}_i^\eta, \tag{2}$$

where f_i^η is the measurement along the i-th LoS in the spectral range η and $\tilde{f}_i^\eta$ is perturbative noise (2% Gaussian noise assumed here). The figure of merit RMS_{SXR} to minimize in order to find ($T_{e,0}$, $c_{W,0}$) candidates compatible with N_f measurements is defined as:

$$RMS_{SXR}\left(c_{W,0}, T_{e,0}\right) = \frac{1}{\max\left(f_{i,meas}\right)} \sqrt{\frac{1}{N_f}\sum_{i=1}^{N_f}\left(f_i\left(c_{W,0}, T_{e,0}\right) - f_{i,meas}\right)^2}, \tag{3}$$

where $f_i(c_{W,0}, T_{e,0})$ are the measurements expected in the $(c_{W,0}, T_{e,0})$ scenario, assuming that radial shapes are known, and $f_{i,meas}$ are the measurements of reference. Such RMS_{SXR} map is established in our synthetic case and shown in Fig. 3. Visibly, each spectral range defines a curve $T_{e,0} = f(c_{W,0})$ of compatible plasma parameters and the crossing of these curves in different energy ranges allow recovering the original scenario $(c_{W,0}, T_{e,0}) = (10^{-4}, 3.0\ keV)$.

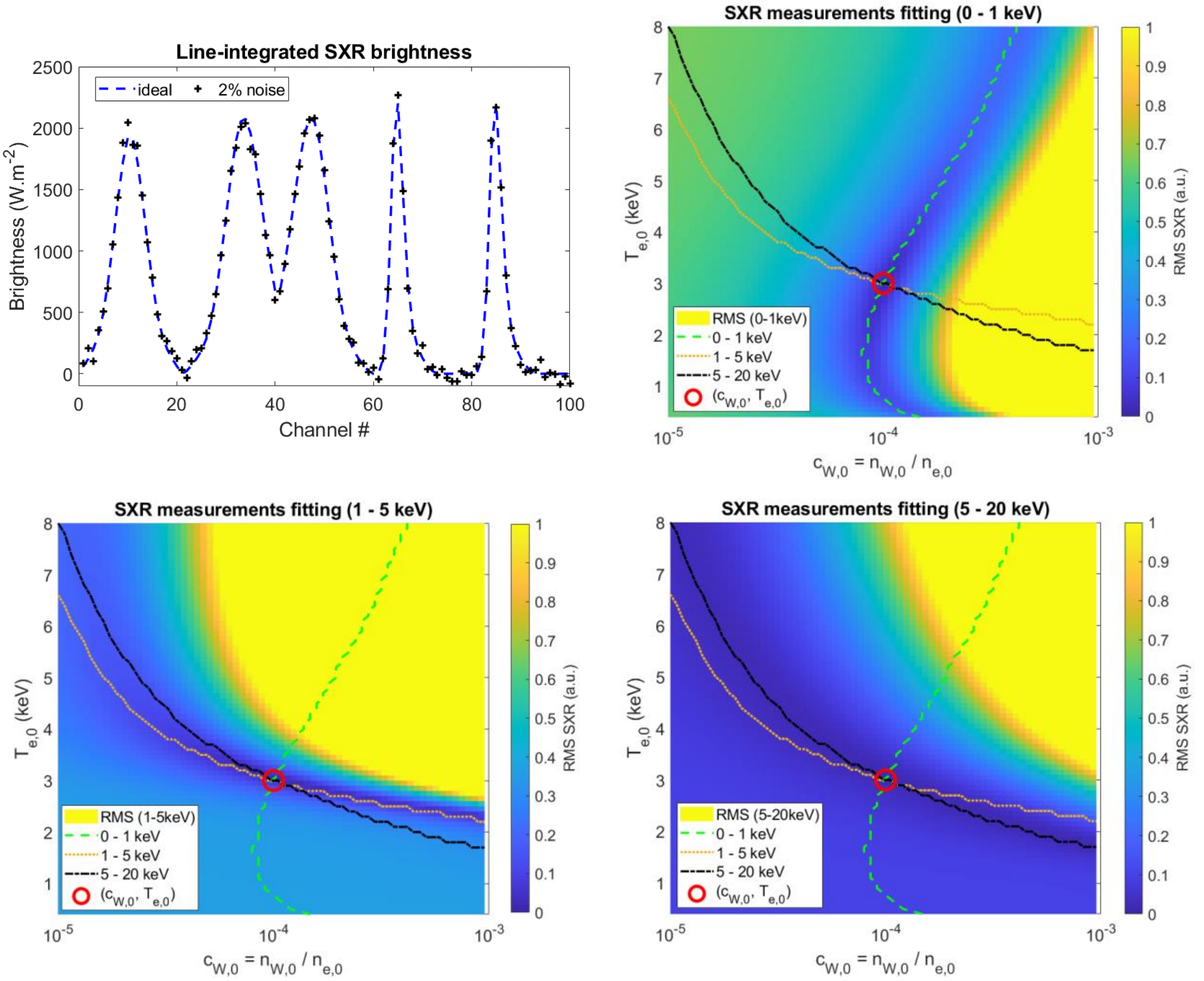

Figure 3. Synthetic SXR brightness in the range 1 - 5keV and RMS SXR error maps for the three spectral ranges 0 - 1 keV, 1 - 5 keV and 5 – 20 keV.

A first experimental test is presented for the WEST discharge #54981 @6.5s, see Fig. 4. The RMS_{SXR} map is performed thanks to the DTOMOX horizontal camera measurements. One can see that while a central temperature below 2 keV is unlikely regardless the $c_{W,0}$ value, a temperature above 4 keV would require a very low amount of W impurities. The HXR measurements are used as a second diagnostic to cross-check SXR information, however since the use of the C3PO-LUKE-R5X2 chain of codes [6] makes it computationally challenging to establish a full $(c_{W,0}, T_{e,0})$ map, only selected scenarios were considered as in [1] and the result of the optimisation is presented in Fig. 4 (black square).

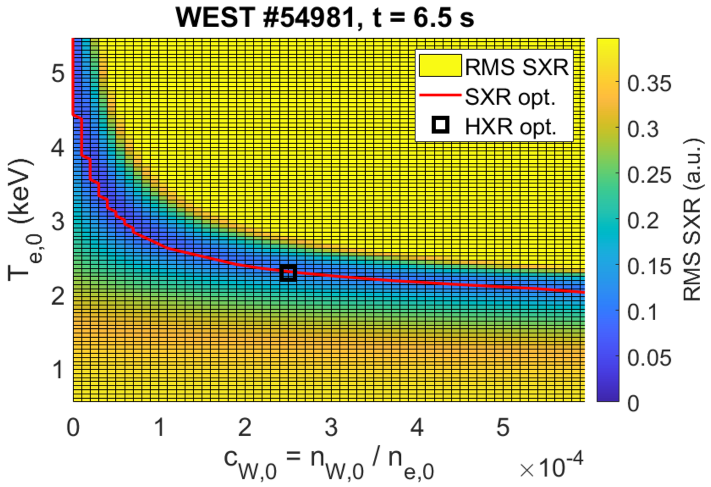

Figure 4. SXR RMS error map for WEST #54981 @t = 6.5s and result of the HXR optimisation.

In summary, it has been shown that X-ray line integrated measurements can be used in different energy bands to estimate both $c_{W,0}$ and $T_{e,0}$ in tokamak plasmas. The methodology has been tested with synthetic profiles, and preliminary tests have been performed with experimental WEST data in the SXR and HXR range. A similar exercise has been recently performed with bolometry/SXR and combined with tomographic inversions to recover radial profiles [7]. This methodology opens promising perspectives for tomography diagnostics that exhibit energy resolution capabilities, such as Gas Electron Multiplier (GEM) detectors [8].

References

[1] D. Mazon, et al (2022) JINST 17 C01073.

[2] T. Pütterich et al (2010) Nucl. Fusion 50 025012.

[3] A. Jardin et al (2021) Eur. Phys. J. Plus 136:706.

[4] P. V. Subhash et al (2017) Fusion Sci. Technol. 72 49–59.

[5] The Open ADAS Project (Atomic Data and Analysis Structure). http://open.adas.ac.uk.

[6] Y Peysson et al (2016) Plasma Phys. Control. Fusion 58 044008.

[7] P. Manas et al (2023) WEST TFM, March 2023.

[8] D. Mazon et al (2023) in proceedings of the 49th EPS conference on Plasma Physics.

Acknowledgements

This work has been partially funded by the National Science Centre, Poland (NCN) grant HARMONIA 10 no. 2018/30/M/ST2/00799. We gratefully acknowledge Poland’s high-performance computing infrastructure PLGrid (HPC Centers: ACK Cyfronet AGH) for providing computer facilities and support within computational grant no. PLG/2022/015994. This work has been carried out within the framework of the EUROfusion Consortium, funded by the European Union via the Euratom Research and Training Programme (Grant Agreement No 101052200 — EUROfusion). Views and opinions expressed are however those of the authors only and do not necessarily reflect those of the European Union or the European Commission. Neither the European Union nor the European Commission can be held responsible for them. This work has been published in the framework of the international project co-financed by the Polish Ministry of Education and Science, as program “PMW”.